Collaborative Tracking and Positioning of Unmanned Aerial Vehicles Over Wireless Sensor Networks

Xingzhen Bai, Liqun Yu, Guhui Li, Lu Liu and Xiao Chen

***Abstract*—In recent years, wireless sensor networks have been widely applied in information acquisition and real-time monitoring of consumer electronics, particularly for tracking and positioning of consumer unmanned aerial vehicles (UAVs) in outdoor rescue scenarios. However, the challenging outdoor environments introduce reliability and security concerns in the sensor data acquisition process, and there remains a significant gap in related research efforts. To address this issue, this paper introduces an amplify-and-forward relaying strategy to ensure dependable signal transmission, while a residual saturation mechanism is applied to tackle randomly occurring measurement outliers. Additionally, a recursive extended Kalman filter is developed for target tracking to address the challenge of UAVs positioning within wireless sensor networks. The efficacy of the proposed filtering algorithm is validated through simulations of UAV target positioning. When compared with alternative methods, the proposed approach demonstrates superior accuracy in UAV positioning.**

***Index Terms*—Unmanned aerial vehicle, wireless sensor networks, recursive extended Kalman filter, amplify-and-forward relay, measurement outliers.**

I. INTRODUCTION

As wireless communication technology evolves and 5G networks become more widespread, unmanned aerial vehicles (UAVs) serve as essential communication terminals in the consumer electronics market [1]-[3]. UAVs have been extensively employed for tasks such as camera operations [4], delivery services [5], and security surveillance [6]. Notably, urban areas are witnessing a rise in fire incidents, necessitating innovative solutions in firefighting and rescue operations as traditional methods struggle to address the complexities of modern scenarios [7]. UAVs can provide a promising solution by leveraging aerial camera transmission technology to relay real-time feedback and location data to fire scene monitoring platforms [8], [9]. Despite their significant potential, navigating complex rescue environments, characterized by obstacles, signal interference, and unforeseen conditions, presents considerable challenges to UAV positioning [10]. Therefore, there is practical engineering significance in developing an accurate UAV positioning method to improve positioning accuracy and anti-interference capabilities in complex environments.

Up to now, various UAV positioning techniques have been researched, including, but not limited to, global positioning systems (GPS), inertial navigation systems (INS), vision/lidar positioning [11], integrated GPS/INS positioning [12], and wireless sensor network techniques [13]. INS positioning methods, in particular, inherently introduce integration bias, leading to dispersed results. Moreover, GPS signals are vulnerable to interference from tall buildings in urban environments, resulting in significant fading and multipath effects, thereby increasing positioning errors significantly [14]. Recently, wireless sensor network-based positioning approaches have been widely investigated and applied in the field of consumer electronics, offering significant advantages such as high accuracy, low cost, and increased flexibility [15]-[18]. For example, a wireless sensor network-based UAV positioning scheme has been used to achieve real-time closed-loop estimation of the target's position and velocity during flying and hovering, while considering GPS signal rejection in indoor environments [19]. Additionally, by combining the dipole antenna with terrestrial sensor network radio frequency positioning, the positioning accuracy has been improved, uncovering a non-monotonic relationship between UAV flight altitude and positioning performance [20].

Rescue UAVs usually operate in intricate environments, where measurement noises and interferences are unavoidable during the UAV positioning process [21]-[23]. In such scenarios, filtering techniques in the Kalman framework are extensively employed to attain precise UAV positioning information. While the Kalman filter effectively addresses linear systems [24], its applicability diminishes for nonlinear models. As such, the extended Kalman filter (EKF) has been extensively researched to tackle nonlinearities. For example, a framework for UAV navigation with asynchronous cellular signals has been proposed, employing an EKF algorithm to estimate the position and velocity of the UAV, along with the deviation and drift between the receiver's and each base station's clock [25]. Furthermore, an EKF has been introduced to eliminate noises in UAV navigation systems, incorporating the Rauch-Tung-Striebel smoothing method to improve the linearized reference point and reduce truncation errors [26]. Nevertheless, the EKF ignores higher-order terms in the

This work was supported in part by the National Natural Science Foundation of China under Grant 62273211. *(Corresponding author: Lu Liu.)*

Xingzhen Bai, Liqun Yu and Guhui Li are with the School of Electrical and Automation Engineering, Shandong University of Science and Technology, Qingdao 266590, China (e-mail: xzbai@163.com; yulq0808@163.com; lgh_sdust@163.com).

Lu Liu is with the Department of Computer Science, University of Exeter, Exeter, EX4 4RN, UK (email: l.liu3@exeter.ac.uk).

Xiao Chen is with the School of Computing and Mathematical Science, University of Leicester, Leicester LE1 7RH, UK (e-mail: xiao.chen@leicester.ac.uk).

TABLE I
OUTLIER-RESISTANT METHODS AND RELAYING STRATEGIES USED BY EXISTING WORKS

	Ref	Research subject	Approaches used	Drawbacks
Outlier-resistant methods	[30]	Multi-machine power systems	Sliding window-based online algorithm	Complex algorithms with long running times
	[31]	Mobile robot localization	Adaptive saturation boundary	Complex implementation with low reliability
	[32]	Delayed complex networks	Multiple-order-holder approach	Difficult to calculate
Relaying strategies	[35]	Two-dimensional target tracking	Filter-and-forward relays	Complex structure and difficult to realize
	[36]	Multiple-input multiple-output systems	Decode-and-forward relays	Decoding errors and high energy consumption
	[37]	Cloud radio-access network	Compress-and-forward relays	Technically complex

Taylor expansion, which may seriously impact filtering performance and even result in the dispersion of filtering results. Consequently, scholars have proposed the recursive extended Kalman filter (REKF) algorithm to address this limitation. This algorithm enhances filtering properties by representing the linearization error in terms of an uncertainty matrix [27]. Given this situation, a natural idea is to utilize the REKF to achieve a more accurate estimation of the real trajectories of UAVs.

In addition to measurement noises during data acquisition, measurements may also undergo sudden, large changes randomly, known as measurement outliers, due to factors such as complex environmental disturbances and measurement device failures [28]. Unlike the widely studied Gaussian white noises, measurement outliers, characterized by large amplitude and random occurrence, can significantly interfere with and misinform filter design and analysis [29], thus impacting the tracking performance of the UAV location system. To address challenges, filtering problems subject to measurement outliers have received extensive attention. Particularly, the authors of [30] have proposed a sliding window-based online algorithm to detect and localize outliers with historical data. The concept of a saturated boundary has been introduced, which saturates an innovation when distorted by outliers, preventing innovations from compromising the state estimation process [31]. Additionally, a multi-order hold approach has been proposed to mitigate the influence of intermittent measurement outliers by applying a weighted average of the previously normal data [32].

In practical engineering, wireless transmission signals are sent from measurement base stations to the remote monitoring center via a complex communication channel. Factors such as distance limitations, sensor energy constraints, and building obstructions contribute to the signal attenuation and distortion [33], potentially causing valid information to fail to reach the remote monitoring center directly. To address this issue, the relay communication strategy provides an effective solution. In this strategy, signals from the measurement base station are amplified and forwarded to the monitoring center by the relay nodes [34], ensuring the quality of information transmission. To improve system performance, a filter-and-forward relaying strategy has been proposed, where local filters are constructed at each relay for state estimation and then fused at the remote estimator [35]. Additionally, to improve confidentiality, the decode-and-forward relaying method has been proposed, reducing the risk of the signal interception by eavesdroppers to a certain extent [36]. Another approach, the compress-and-forward relaying strategy, forwards the measurement signals to the remote site after precoding and compression. Users then receive the data through decompression and decoding, which improves the end-to-end rate [37]. However, the introduction of the relaying strategy may increase the complexity of the filtering algorithm design.

The problem of state estimation in wireless sensor networks has been extensively studied, and a comparison of existing outlier-resistant methods and relaying strategies is shown in Table I. Despite this, most existing studies have overlooked the impact of intricate factors in practical engineering, such as long-distance transmission and randomly occurring measurement outliers. Given these intricate scenarios, traditional UAV positioning methods often fall to provide accurate positioning results. Consequently, the primary objective of this paper is to design a REKF algorithm tailored for UAV wireless positioning systems, considering measurement outliers and relaying transmissions to achieve accurate UAV positioning and enhance the efficacy of urban rescue operations. The key technical contributions of this paper are as follows:

1) An amplify-and-forward (AF) relaying strategy is introduced in the transmission of UAV signals to ensure distortion-free transmission.

2) An innovative saturation mechanism is employed to

eliminate measurement outliers, without requiring any a priori knowledge or assumptions about such outliers.

3) The UAV target positioning problem is investigated, for the first time, in the presence of relay communications and measurement outliers within a wireless sensor network framework.

4) A suitable REKF algorithm is proposed specifically for the positioning of rescue UAVs in complex settings, facilitating online applications and precise tracking of target position and velocity.

The remainder of this paper is organized as follows. In Section II, the network structure and the dynamic system model are briefly introduced, and the outlier-resistant saturation function and the AF relaying scheme are described. In Section III, the REKF with outliers and relay mechanism is designed. Simulation results are presented in Section IV. Finally, we conclude this paper in Section V.

II. Problem Formulation

A. Network structure of UAV wireless positioning system

Considering the necessity for reliable monitoring in practical applications, the monitoring area is typically divided into several sub-regions. In each sub-region, wireless sensor nodes are strategically deployed. In a sensor network sub-region consisting of $m+1$ sensors, where the i th sensor is positioned at a known location as a reference node, the time delay of arrival (TDOA) positioning method is applied to determine the UAV position, as shown in Fig. 1.

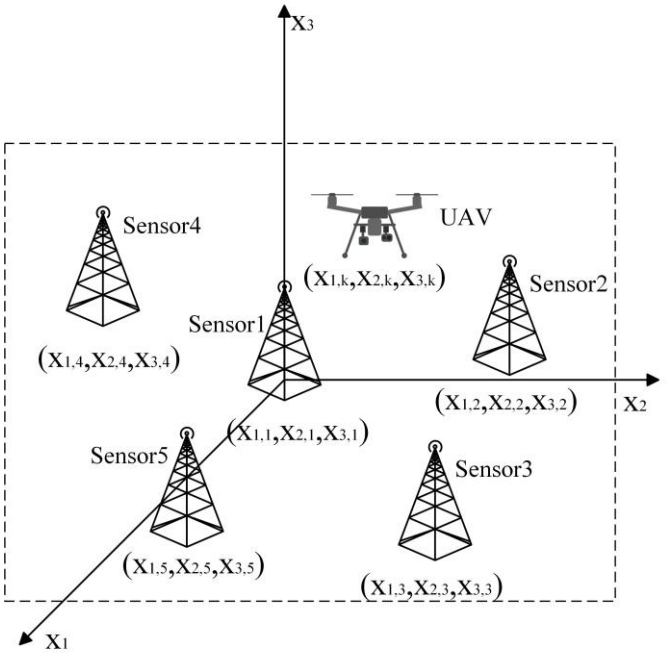

Fig. 1. TDOA measurements are collected within the sensor network sub-region for wireless positioning.

B. System model

In this section, the target is regarded as moving within a three-dimensional monitoring area, and its state vector is denoted as $x_k = \begin{bmatrix} x_{1,k} & \upsilon_{1,k} & x_{2,k} & \upsilon_{2,k} & x_{3,k} & \upsilon_{3,k} \end{bmatrix}^T \in \mathbb{R}^n$, where $x_{i,k} \in \mathbb{R}$ and $\upsilon_{i,k} \in \mathbb{R}$ $(i = 1,2,3)$ signify the position and velocity along the x_i -axis at the time t_k, respectively. Based on the actual motion characteristics of the UAV, the system model is formulated as

$$x_{k+1} = A_k x_k + B_k u_k + \omega_k \tag{1}$$

where

$$A_k = \begin{bmatrix} 1 & T_k & 0 & 0 & 0 & 0 \\ 0 & 1 & 0 & 0 & 0 & 0 \\ 0 & 0 & 1 & T_k & 0 & 0 \\ 0 & 0 & 0 & 1 & 0 & 0 \\ 0 & 0 & 0 & 0 & 1 & T_k \\ 0 & 0 & 0 & 0 & 0 & 1 \end{bmatrix}, \; B_k = \begin{bmatrix} \frac{T_k^2}{2} & 0 & 0 \\ T_k & 0 & 0 \\ 0 & \frac{T_k^2}{2} & 0 \\ 0 & T_k & 0 \\ 0 & 0 & \frac{T_k^2}{2} \\ 0 & 0 & T_k \end{bmatrix}.$$

The $T_k = t_{k+1} - t_k$ denotes the time interval between two consecutive sampling moments, and the control quantity $u_k = [u_{1,k} \quad u_{2,k} \quad u_{3,k}]^T$ denotes the acceleration of the UAV motion with $u_{i,k}$ representing the acceleration along the x_i -axis. Furthermore, B_k designates the weights associated with distinct accelerations, and $\omega_k \in \mathbb{R}^n$ represents the process noise. In addition, the measurement model for the a th sensor node at time t_k is given by

$$y_{a,k} = g_a(x_k) + v_k^a \tag{2}$$

where $y_{a,k}$ denotes the measurement, v_k^a represents the measurement noise, and $g_a(x_k)$ is defined as

$$g_a(x_k) = \sqrt{(x_{1,k} - x_{1,a}^*)^2 + (x_{2,k} - x_{2,a}^*)^2 + (x_{3,k} - x_{3,a}^*)^2} - \sqrt{(x_{1,k} - x_{1,i}^*)^2 + (x_{2,k} - x_{2,i}^*)^2 + (x_{3,k} - x_{3,i}^*)^2}$$

where $x_{1,a}^*$, $x_{2,a}^*$, and $x_{3,a}^*$ stand for the coordinate values of the a th sensor node along the x_1 -axis, x_2 -axis and x_3 -axis, respectively; moreover, $x_{1,i}^*$, $x_{2,i}^*$ and $x_{3,i}^*$ denote the coordinates of the reference sensor node. To simplify the notation, let us represent

$$g(x_k) = [g_1(x_k) \quad g_2(x_k) \quad \ldots \quad g_m(x_k)]^T,$$
$$v_k = \begin{bmatrix} v_k^1 & v_k^2 & \ldots & v_k^m \end{bmatrix}^T,$$
$$y_k = \begin{bmatrix} y_{1,k} & y_{2,k} & \ldots & y_{m,k} \end{bmatrix}^T.$$

Then, we have

$$y_k = g(x_k) + v_k. \tag{3}$$

In this paper, the system noise ω_k and the measurement noise v_k are modeled as Gaussian noises with zero mean and variances Q_k and R_k, respectively.

Remark 1: In this paper, wireless sensor nodes are

strategically deployed across a designated monitoring area to address the UAV positioning problem. Sensors positioned within the same area collaborate to sense the target's position when the UAV enters their region, thereby enhancing the reliability of target state estimation. In addition, the UAV periodically transmits signals to the sensors through the wireless radio frequency channel and tracks the target's position with the TDOA positioning method. This method is chosen for its capacity to minimize errors introduced by clock asynchrony [38].

C. AF relaying strategy

In practical engineering, signals transmitted from energy-limited sensors to the remote monitoring center via wireless links may experience distortion over long distances due to fading. To ensure high-quality signal transmission, AF relays are incorporated between the sensor nodes and the monitoring center. These relays receive signals from the sensors and forward them to the destination. Let z_k denote the signals received by the relays in the following form:

$$z_k = \sqrt{P_{s,k}} C_{s,k} y_k + \vartheta_{s,k} \tag{4}$$

where $P_{s,k}$ denotes the average signal energy received by the relays, corresponding to the transmitted power of the sensors, $C_{s,k}$ denotes the channel gain between the sensors and the relays, and $\vartheta_{s,k}$ is an additive zero-mean Gaussian white noise with variance $E\{\vartheta_{s,k}\vartheta_{s,k}^T\} = S_{s,k}$.

Upon receiving signals from the sensors, the relays amplify and forward them to the remote monitoring center for filtering. The measurements received at the filter can be characterized as

$$r_k = \sqrt{P_{r,k}} C_{r,k} z_k + \vartheta_{r,k} \tag{5}$$

where $P_{r,k}$ denotes the average signal energy received by the filter, corresponding to the transmitted power of the relays, $C_{r,k}$ denotes the channel gain between the relays and the filter, and $\vartheta_{r,k}$ is an additive zero-mean Gaussian white noise with variance $E\{\vartheta_{r,k}\vartheta_{r,k}^T\} = S_{r,k}$.

Assumption 1: The random variables ω_k, v_k, x_0, $\vartheta_{s,k}$ and $\vartheta_{r,k}$ are mutually uncorrelated.

Remark 2: In this paper, ω_k is used to describe the unmodelled dynamics of the system model, v_k is considered to represent the measurement error of the sensors, $\vartheta_{s,k}$ and $\vartheta_{r,k}$ are introduced to characterize the external interference to the channel. Typically, these noises are assumed to be independent of each other and not dependent on the state initials x_0, and such an assumption is consistent with practical engineering [31].

Remark 3: To ensure distortion-free signal transmission over extended distances, this paper introduces an AF relaying strategy instead of relying on simple channel transmission models like Rayleigh or Rician fading. The integration of the AF relaying technique addresses issues pertaining to sensor transmission power limitations and long-distance signal transmission [39]. With this scheme, the relay functions as an intermediary link that amplifies the received signal before forwarding it to the filter. Nevertheless, the utilization of relays also introduces complexities to the signal transmission process, adding a challenge to the filter design.

D. Outlier-resistant filter design

Measurements frequently exhibit deviations from normal values due to abnormal disturbances, and if left unaddressed, these deviations may lead to significant deviations or even discrete outcomes. To mitigate the adverse effects of outliers, a saturation function is introduced in this paper to eliminate outliers by restricting the range of innovation. Based on the system model (1), the outlier-resistant filter is constructed as follows:

$$\hat{x}_{k+1|k} = A_k \hat{x}_{k|k} + B_k u_k, \tag{6}$$

$$\hat{x}_{k+1|k+1} = \hat{x}_{k+1|k} + K_{k+1}\sigma(\tilde{r}_{k+1}) \tag{7}$$

where $\hat{x}_{k+1|k}$ and $\hat{x}_{k+1|k+1}$ represent the one-step prediction and estimation of the state at the instant $k+1$, respectively, and K_{k+1} is the designed filter gain. Here, the saturation function $\sigma(\cdot): \square \to \square$ is defined as follows:

$$\sigma(\tilde{r}_{k+1}) \square sign(\tilde{r}_{k+1}) \min\{\tilde{r}_{k+1}^{\max}, |\tilde{r}_{k+1}|\} \tag{8}$$

where

$$\tilde{r}_{k+1} = r_{k+1} - \sqrt{P_{s,k+1}}\sqrt{P_{r,k+1}} C_{s,k+1} C_{r,k+1} g(\hat{x}_{k+1|k})$$

is the innovation and $\tilde{r}_{k+1}^{\max}$ is the innovation saturation constraint bound.

Remark 4: The innovations are restricted within the saturation boundaries $\tilde{r}_{k+1}^{\max}$ by introducing a saturation function, thereby reducing the impact of measurement outliers on the filtering results. The saturation bound $\tilde{r}_{k+1}^{\max}$ is determined based on prior knowledge in engineering practice. In this context, the saturation function $\sigma(\cdot)$ is contingent on confidence-dependent, affirming the outlier-resistant nature of the filter.

Define the one-step prediction error and filtering error, as $\tilde{x}_{k+1|k} \square x_{k+1} - \hat{x}_{k+1|k}$ and $\tilde{x}_{k+1|k+1} \square x_{k+1} - \hat{x}_{k+1|k+1}$, respectively. Then, according to the formulated filter (6)-(7), $\tilde{x}_{k+1|k}$ and $\tilde{x}_{k+1|k+1}$ can be respectively represented as

$$\tilde{x}_{k+1|k} = A_k \tilde{x}_{k|k} + \omega_k, \tag{9}$$

$$\tilde{x}_{k+1|k+1} = \tilde{x}_{k+1|k} - K_{k+1}\sigma(\tilde{r}_{k+1}). \tag{10}$$

Considering the collaborative impact of the AF relaying transmission and measurement outliers, the main objective of this paper is to devise an outlier-resistant filter in the form of equations (6)-(7), aiming to:

1) the upper bound on the filtering error covariance $\Xi_{k+1|k+1}$

is guaranteed, i.e., $\Xi_{k+1|k+1} \le \bar{\Xi}_{k+1|k+1}$; and

2) the filter gain K_{k+1} is obtained at each moment by minimizing the upper bound $\bar{\Xi}_{k+1|k+1}$.

III. Main Results

Based on the implemented AF relaying scheme, the developed outlier-resistant mechanism, and the formulated filter structure, this section explores the design of a REKF tailored for time-varying systems with AF relaying transmission and measurement outliers. A sufficient condition is established for the presence of an upper bound on the filtering error covariance, which is then minimized to determine an appropriate filter gain.

Firstly, let us recall the following lemmas, which will be used in the subsequent developments.

Lemma 1: For any given vectors $X, Y \in \mathbb{R}^n$ and a positive scalar $\varepsilon > 0$, the following inequality holds [40]:

$$XY^T + YX^T \le \varepsilon XX^T + \varepsilon^{-1} YY^T. \tag{11}$$

Lemma 2: For any given matrices F, H, W, and Y with appropriate dimensions satisfying $YY^T \le I$, let T be a symmetric positive definite matrix and δ be an arbitrary positive constant such that $\delta^{-1} I - WTW^T > 0$. Then, the following inequality holds [41]:

$$\begin{aligned}&(F+HYW)T(F+HYW)^T\\ &\quad\le F(T^{-1}-\delta W^T W)^{-1}F^T + \delta^{-1}HH^T.\end{aligned} \tag{12}$$

It is evident that, despite the concept of the outlier-resistant mechanism being clearly described by (8), the saturation function $\sigma(\cdot)$ poses challenges in its application to filter design. To facilitate further the filter design, an uncertainty diagonal matrix Φ_k is introduced to identify the moment of outlier occurrences, thereby introducing an alternative form of the saturation function $\sigma(\cdot)$ as shown in (15).

For any positive scalars a and b, define the following scalar function:

$$f(a,b) \triangleq \begin{cases} 0, & if \quad a \le b; \\ 1, & otherwise, \end{cases} \tag{13}$$

then the function (8) can be rewritten as

$$\begin{aligned}\sigma(\tilde{r}_k) &= \left[1 - f(|\tilde{r}_k|, \tilde{r}_k^{\max})\right]\tilde{r}\\ &\quad + f(|\tilde{r}_k|, \tilde{r}_k^{\max})\tilde{r}_k^{\max} sign(\tilde{r}_k),\end{aligned} \tag{14}$$

which yields

$$\sigma(\tilde{r}_k) = (I - \Phi_k)\tilde{r}_k + \Phi_k \Gamma_k \tag{15}$$

where I is an identity matrix of appropriate dimension,

$$\begin{aligned}\Phi_k &\triangleq diag\{f(|\tilde{r}_{1,k}|, \tilde{r}_k^{\max}), f(|\tilde{r}_{2,k}|, \tilde{r}_k^{\max}),\\ &\quad \dots, f(|\tilde{r}_{m,k}|, \tilde{r}_k^{\max})\},\\ \Gamma_k &\triangleq col\{\tilde{r}_{1,k}^{\max} sign(\tilde{r}_{1,k}), \tilde{r}_{1,k}^{\max} sign(\tilde{r}_{1,k}),\\ &\quad \dots, \tilde{r}_{m,k}^{\max} sign(\tilde{r}_{m,k})\}.\end{aligned}$$

By introducing a novel saturation function to restrain the innovations to a saturation value $\tilde{r}^{\max}$, the saturated innovations $\sigma(\tilde{r}_k)$, are subsequently expressed as linear combinations of the saturation value and the innovations, facilitating further parameterization.

From (15) and (10), the filtering error can be rewritten as

$$\tilde{x}_{k+1|k+1} = \tilde{x}_{k+1|k} - K_{k+1}(I - \Phi_{k+1})\tilde{r}_{k+1} - K_{k+1}\Phi_{k+1}\Gamma_{k+1}. \tag{16}$$

Expand $g(x_{k+1})$ in a Taylor series around $\hat{x}_{k+1|k}$,

$$g(x_{k+1}) = g(\hat{x}_{k+1|k}) + (G_{k+1} + C_{k+1}\Delta_{k+1}L_{k+1})\tilde{x}_{k+1|k} \tag{17}$$

where, $G_{k+1} \triangleq \partial g(x_{k+1})/\partial x_{k+1}|_{x=\hat{x}_{k+1|k}}$, C_{k+1} and L_{k+1} are bounded matrices, and the unknown time-varying matrix L_{k+1} satisfies $L_{k+1}L_{k+1}^T \le I$ accounting for the linearization error.

Given that the saturation function $\sigma(\cdot)$ influences the innovations, directly obtaining the precise value of the error covariance becomes challenging due to the involvement of the uncertainty matrix. Therefore, we turn to its upper bound for estimation purposes. The upper bound $\bar{\Xi}_{k+1|k+1}$ of the filtering error covariance $\Xi_{k+1|k+1}$ is derived from the filtering error $\tilde{x}_{k+1|k+1}$, and then the filter gain K_{k+1} that minimizes the upper bound $\bar{\Xi}_{k+1|k+1}$ is obtained to complete the filter design.

Theorem 1: Given the system model (1) and (5), as well as the filter (6)-(7), there exist positive scalars ε_1, ε_2, ε_3, γ_1, and γ_2 such that the upper bound $\bar{\Xi}_{k+1|k+1}$ on the filtering error covariance is designed as follows:

$$\bar{\Xi}_{k+1|k} = A_k \bar{\Xi}_{k|k} A_k^T + Q_k, \tag{18}$$

$$\begin{aligned}&\bar{\Xi}_{k+1|k+1}\\ &= a_1((I - K_{k+1}F_{k+1}G_{k+1})(\bar{\Xi}_{k+1|k}^{-1} - \gamma_1 L_{k+1}^T L_{k+1})^{-1}\\ &\times(I - K_{k+1}F_{k+1}G_{k+1})^T + \gamma_1^{-1}K_{k+1}F_{k+1}C_{k+1}(K_{k+1}F_{k+1}\\ &\times C_{k+1})^T) + a_2 tr\{K_{k+1}F_{k+1}G_{k+1}(\bar{\Xi}_{k+1|k}^{-1} - \gamma_2 L_{k+1}^T L_{k+1})^{-1}\\ &\times(K_{k+1}F_{k+1}G_{k+1})^T + \gamma_2^{-1}K_{k+1}F_{k+1}C_{k+1}(K_{k+1}F_{k+1}C_{k+1})^T\}I\\ &+a_3 n_z(\tilde{r}^{\max})^2 K_{k+1}K_{k+1}^T + tr\{K_{k+1}F_{k+1}R_{k+1}(K_{k+1}F_{k+1}\\ &\times R_{k+1})^T\}I + P_{r,k+1}K_{k+1}tr\{C_{r,k+1}R_{s,k+1}C_{r,k+1}^T\}IK_{k+1}^T\\ &+K_{k+1}tr\{R_{r,k+1}\}IK_{k+1}^T\end{aligned} \tag{19}$$

where

$$\begin{aligned}a_1 &\triangleq 1 + \varepsilon_1 + \varepsilon_2,\\ a_2 &\triangleq 1 + \varepsilon_1^{-1} + \varepsilon_3,\\ a_3 &\triangleq 1 + \varepsilon_2^{-1} + \varepsilon_3^{-1}.\end{aligned}$$

Proof: According to (16), the filtering error is rewritten as

$$\begin{aligned}\tilde{x}_{k+1|k+1} &= (I - K_{k+1}F_{k+1}\Psi_{k+1})\tilde{x}_{k+1|k}\\ &\quad + K_{k+1}\Phi_{k+1}F_{k+1}\Psi_{k+1}\tilde{x}_{k+1|k}\\ &\quad - K_{k+1}F_{k+1}(I - \Phi_{k+1})V_{k+1} - K_{k+1}\Phi_{k+1}\Gamma_{k+1}\\ &\quad - \sqrt{P_{r,k+1}}K_{k+1}(I - \Phi_{k+1})C_{r,k+1}\vartheta_{s,k+1}\\ &\quad - K_{k+1}(I - \Phi_{k+1})\vartheta_{r,k+1}\end{aligned} \tag{20}$$

where

$$F_{k+1} \triangleq \sqrt{P_{s,k+1}}\sqrt{P_{r,k+1}}C_{s,k+1}C_{r,k+1},$$

$$\Psi_{k+1} \triangleq G_{k+1} + C_{k+1}\Delta_{k+1}L_{k+1}.$$

From the definitions of the one-step prediction error covariance $\Xi_{k+1|k} \triangleq E\{\tilde{x}_{k+1|k}\tilde{x}_{k+1|k}^T\}$ and the filtering error covariance $\Xi_{k+1|k+1} \triangleq \mathrm{E}\{\tilde{x}_{k+1|k+1}\tilde{x}_{k+1|k+1}^T\}$, it is obtained that

$$\Xi_{k+1|k} = A_k\Xi_{k|k}A_k^T + Q_k, \tag{21}$$

$$\begin{aligned}
&\Xi_{k+1|k+1}\\
&= E\{(I-K_{k+1}F_{k+1}\Psi_{k+1})\tilde{x}_{k+1|k}((I-K_{k+1}F_{k+1}\Psi_{k+1})\\
&\times\tilde{x}_{k+1|k})^T\} + E\{K_{k+1}\Phi_{k+1}F_{k+1}\Psi_{k+1}\tilde{x}_{k+1|k}(K_{k+1}\Phi_{k+1}F_{k+1}\\
&\times\Psi_{k+1}\tilde{x}_{k+1|k})^T\} + E\{K_{k+1}F_{k+1}(I-\Phi_{k+1})V_{k+1}(K_{k+1}F_{k+1}\\
&\times(I-\Phi_{k+1})V_{k+1})^T\} + P_{r,k+1}E\{K_{k+1}(I-\Phi_{k+1})C_{r,k+1}\vartheta_{s,k+1}\\
&\times(K_{k+1}(I-\Phi_{k+1})C_{r,k+1}\vartheta_{s,k+1})^T\} + E\{K_{k+1}\Phi_{k+1}\Gamma_{k+1}\\
&\times(K_{k+1}\Phi_{k+1}\Gamma_{k+1})^T\} + E\{K_{k+1}(I-\Phi_{k+1})\vartheta_{r,k+1}(K_{k+1}\\
&\times(I-\Phi_{k+1})\vartheta_{r,k+1})^T\} + S_{1,k+1} + S_{1,K+1}^T - S_{2,k+1} - S_{2,k+1}^T\\
&-S_{3,k+1} - S_{3,k+1}^T
\end{aligned} \tag{22}$$

where

$$\begin{aligned}
S_{1,k+1} &\triangleq E\{(I-K_{k+1}F_{k+1}\Psi_{k+1})\tilde{x}_{k+1|k}\\
&\quad\times(K_{k+1}\Phi_{k+1}F_{k+1}\Psi_{k+1}\tilde{x}_{k+1|k})^T\},\\
S_{2,k+1} &\triangleq E\{(I-K_{k+1}F_{k+1}\Psi_{k+1})\tilde{x}_{k+1|k}(K_{k+1}\Phi_{k+1}\Gamma_{k+1})^T\},\\
S_{3,k+1} &\triangleq E\{K_{k+1}\Phi_{k+1}F_{k+1}\Psi_{k+1}\tilde{x}_{k+1|k}(K_{k+1}\Phi_{k+1}\Gamma_{k+1})^T\}.
\end{aligned}$$

Notice that finding an explicit expression for the filtering error covariance is challenging due to the presence of a complex set of cross-terms. By utilizing Lemma 1, upper bounds for these terms can be derived as follows:

$$\begin{aligned}
&-S_{1,k+1} - S_{1,k+1}^T\\
&\le \varepsilon_1 E\{(I-K_{k+1}F_{k+1}\Psi_{k+1})\tilde{x}_{k+1|k}((I-K_{k+1}F_{k+1}\Psi_{k+1})\\
&\times\tilde{x}_{k+1|k})^T\} + \varepsilon_1^{-1}E\{K_{k+1}\Phi_{k+1}F_{k+1}\Psi_{k+1}\tilde{x}_{k+1|k}\\
&\times(K_{k+1}\Phi_{k+1}F_{k+1}\Psi_{k+1}\tilde{x}_{k+1|k})^T\},
\end{aligned} \tag{23}$$

$$\begin{aligned}
&-S_{2,k+1} - S_{2,k+1}^T\\
&\le \varepsilon_2 E\{(I-K_{k+1}F_{k+1}\Psi_{k+1})\tilde{x}_{k+1|k}((I-K_{k+1}F_{k+1}\Psi_{k+1})\\
&\times\tilde{x}_{k+1|k})^T\} + \varepsilon_2^{-1}E\{K_{k+1}\Phi_{k+1}\Gamma_{k+1}(K_{k+1}\Phi_{k+1}\Gamma_{k+1})^T\},
\end{aligned} \tag{24}$$

$$\begin{aligned}
&S_{3,k+1} + S_{3,k+1}^T\\
&\le \varepsilon_3 E\{K_{k+1}\Phi_{k+1}F_{k+1}\Psi_{k+1}\tilde{x}_{k+1|k}(K_{k+1}\Phi_{k+1}F_{k+1}\Psi_{k+1}\\
&\times\tilde{x}_{k+1|k})^T\} + \varepsilon_3^{-1}E\{K_{k+1}\Phi_{k+1}\Gamma_{k+1}(K_{k+1}\Phi_{k+1}\Gamma_{k+1})^T\}.
\end{aligned} \tag{25}$$

By exploiting the properties of matrix operations, the following equations hold:

$$\begin{aligned}
&E\{(I-K_{k+1}F_{k+1}\Psi_{k+1})\tilde{x}_{k+1|k}((I-K_{k+1}F_{k+1}\Psi_{k+1})\tilde{x}_{k+1|k})^T\}\\
&\le (I-K_{k+1}F_{k+1}G_{k+1})(\Xi_{k+1|k}^{-1} - \gamma_1 L_{k+1}^T L_{k+1})^{-1}(I-K_{k+1}F_{k+1}\\
&\times G_{k+1})^T + \gamma_1^{-1}K_{k+1}F_{k+1}C_{k+1}(K_{k+1}F_{k+1}C_{k+1})^T,
\end{aligned} \tag{26}$$

$$\begin{aligned}
&E\{K_{k+1}\Phi_{k+1}F_{k+1}\Psi_{k+1}\tilde{x}_{k+1|k}(K_{k+1}\Phi_{k+1}F_{k+1}\Psi_{k+1}\tilde{x}_{k+1|k})^T\}\\
&\le tr\{K_{k+1}F_{k+1}G_{k+1}(\Xi_{k+1|k}^{-1} - \gamma_2 L_{k+1}^T L_{k+1})^{-1}(K_{k+1}F_{k+1}\\
&\times G_{k+1})^T + \gamma_2^{-1}K_{k+1}F_{k+1}C_{k+1}(K_{k+1}F_{k+1}C_{k+1})^T\}I,
\end{aligned} \tag{27}$$

$$\begin{aligned}
&E\{K_{k+1}F_{k+1}(I-\Phi_{k+1})V_{k+1}(K_{k+1}F_{k+1}(I-\Phi_{k+1})V_{k+1})^T\}\\
&\le K_{k+1}tr\{F_{k+1}R_{k+1}F_{k+1}^T\}IK_{k+1}^T,
\end{aligned} \tag{28}$$

$$\begin{aligned}
&E\{K_{k+1}(I-\Phi_{k+1})C_{r,k+1}\vartheta_{s,k+1}(K_{k+1}(I-\Phi_{k+1})C_{r,k+1}\\
&\times\vartheta_{s,k+1})^T\} \le K_{k+1}tr\{C_{r,k+1}R_{s,k+1}C_{r,k+1}^T\}IK_{k+1}^T,
\end{aligned} \tag{29}$$

$$\begin{aligned}
&E\{K_{k+1}(I-\Phi_{k+1})\vartheta_{r,k+1}(K_{k+1}(I-\Phi_{k+1})\vartheta_{r,k+1})^T\}\\
&\le K_{k+1}tr\{R_{r,k+1}\}IK_{k+1}^T,
\end{aligned} \tag{30}$$

$$E\{K_{k+1}\Phi_{k+1}\Gamma_{k+1}\Gamma_{k+1}^T\Phi_{k+1}^TK_{k+1}^T\} \le m(\tilde{r}^{\max})^2K_{k+1}K_{k+1}^T. \tag{31}$$

Substitute (23)-(31) into (22), it is easy to obtain that

$$\begin{aligned}
&\Xi_{k+1|k+1}\\
&\le a_1((I-K_{k+1}F_{k+1}G_{k+1})(\Xi_{k+1|k}^{-1} - \gamma_1 L_{k+1}^T L_{k+1})^{-1}\\
&\times(I-K_{k+1}F_{k+1}G_{k+1})^T + \gamma_1^{-1}K_{k+1}F_{k+1}C_{k+1}(K_{k+1}F_{k+1}\\
&\times C_{k+1})^T) + a_2tr\{K_{k+1}F_{k+1}G_{k+1}(\Xi_{k+1|k}^{-1} - \gamma_2 L_{k+1}^T L_{k+1})^{-1}\\
&\times(K_{k+1}F_{k+1}G_{k+1})^T + \gamma_2^{-1}K_{k+1}F_{k+1}C_{k+1}(K_{k+1}F_{k+1}C_{k+1})^T\}I\\
&+a_3n_z(\tilde{r}^{\max})^2K_{k+1}K_{k+1}^T + tr\{K_{k+1}F_{k+1}R_{k+1}(K_{k+1}F_{k+1}\\
&\times R_{k+1})^T\}I + P_{r,k+1}K_{k+1}tr\{C_{r,k+1}R_{s,k+1}C_{r,k+1}^T\}IK_{k+1}^T\\
&+K_{k+1}tr\{R_{r,k+1}\}IK_{k+1}^T.
\end{aligned} \tag{32}$$

Then, the upper bound of the filtering error covariance $\bar{\Xi}_{k+1|k+1}$ can be obtained from (32). The saturation value $\tilde{r}_{\max}$ and the noise matrices R, R_s, R_r are assumed reasonably based on actual engineering needs during the design process.■

Theorem 2: The filter gain K_{k+1} is obtained by minimizing the upper bound on the filtering error covariance.

$$K_{k+1} = \Omega_{k+1}\Pi_{k+1}^{-1} \tag{33}$$

where

$$\begin{aligned}
\Omega_{k+1} &\triangleq a_1(\bar{\Xi}_{k+1|k}^{-1} - \gamma_1 L_{k+1}^T L_{k+1})^{-1}(F_{k+1}G_{k+1})^T,\\
\Pi_{k+1} &\triangleq a_1(F_{k+1}G_{k+1}(\bar{\Xi}_{k+1|k}^{-1} - \gamma_1 L_{k+1}^T L_{k+1})^{-1}(F_{k+1}G_{k+1})^T\\
&\quad+\gamma_1^{-1}F_{k+1}C_{k+1}(F_{k+1}C_{k+1})^T) + a_2tr\{F_{k+1}G_{k+1}(\bar{\Xi}_{k+1|k}^{-1}\\
&\quad-\gamma_2 L_{k+1}^T L_{k+1})^{-1}(F_{k+1}G_{k+1})^T + \gamma_2^{-1}F_{k+1}C_{k+1}(F_{k+1}C_{k+1})^T\}I\\
&\quad+a_3n_z(\tilde{r}^{\max})^2I + P_{r,k+1}tr\{C_{r,k+1}R_{s,k+1}C_{r,k+1}^T\}I\\
&\quad+tr\{F_{k+1}R_{k+1}F_{k+1}^T\}I + tr\{R_{r,k+1}\}I.
\end{aligned}$$

Proof: The derivative of the upper bound trace of the covariance with respect to the gain can first be obtained as follows:

$$\begin{aligned}
&\frac{\partial tr(\bar{\Xi}_{k+1|k+1})}{\partial K_{k+1}}\\
&= -2a_1(I-K_{k+1}F_{k+1}G_{k+1})(\bar{\Xi}_{k+1|k}^{-1} - \gamma_1 L_{k+1}^T L_{k+1})^{-1}\\
&\times(F_{k+1}G_{k+1})^T + 2a_1\gamma_1^{-1}K_{k+1}F_{k+1}C_{k+1}(F_{k+1}C_{k+1})^T\\
&+2a_2tr\{K_{k+1}F_{k+1}G_{k+1}(\bar{\Xi}_{k+1|k}^{-1} - \gamma_2 L_{k+1}^T L_{k+1})^{-1}(F_{k+1}G_{k+1})^T\\
&+\gamma_2^{-1}K_{k+1}F_{k+1}C_{k+1}(F_{k+1}C_{k+1})^T\}I + 2a_3n_z(\tilde{r}^{\max})^2K_{k+1}\\
&\times K_{k+1}^T + 2K_{k+1}tr\{F_{k+1}R_{k+1}F_{k+1}^T\}I + 2P_{r,k+1}K_{k+1}\\
&\times tr\{C_{r,k+1}R_{s,k+1}C_{r,k+1}^T\}IK_{k+1}^T + 2K_{k+1}tr\{R_{r,k+1}\}IK_{k+1}^T.
\end{aligned} \tag{34}$$

Let $\partial tr(\bar{\Xi}_{k+1|k+1})/\partial K_{k+1} = 0$, the gain that minimizes the

upper bound of the filter is obtained as $K_{k+1}=\Omega_{k+1}\Pi_{k+1}^{-1}$. ■

Remark 5: Up to this point, the upper bound on the filtering error covariance and the filter gain have been obtained by applying Theorems 1 and 2. It is evident that the state estimation can be executed recursively by computing the one-step prediction by using (6), determining the upper bound on the one-step prediction error covariance with (18), calculating the filter gain matrix with (33), establishing the upper bound on the filter error covariance through (19), and finally obtaining the estimate with (7).

Remark 6: Introducing the AF strategy and the outlier-resistant mechanism inevitably poses a challenge to the filter design, where the cross-terms need to be handled appropriately by using known lemmas. Based on this, an upper bound on the filtering error covariance is obtained rather than an accurate one, and a sub-optimal filter gain can be computed. Nevertheless, the deployment of the AF reduces attenuation and interference during signal transmission, thus improving the reliability of data transmission and the accuracy of UAV positioning [42].

Remark 7: In comparison to existing research on UAV positioning, this paper presents several advantages: 1) It addresses the challenge of UAV positioning in the presence of relays and measurement outliers, thereby enhancing the complexity of the measurement model. 2) An outlier-resistant saturation function is introduced to constrain new measurements of interest, thereby minimizing the influence of outliers on estimation results. 3) The paper proposes an outlier-resistant REKF structure to achieve more precise positioning of the target position.

IV. Simulation Results

In this section, we provide an example of UAV positioning with relay communication and measurement outliers to illustrate the effectiveness of the proposed filtering algorithm. To enhance the reliability of urban firefighting and rescue operations, a wireless sensor network was deployed on the ground for real-time positioning of UAVs. Comprising five sensors responsible for tracking the target in the specified area, the measurements are collectively transmitted to the relays. The relays amplify and forward the measurements to the filter, facilitating the estimation of the target's position to aid in rescue efforts.

In this simulation, the positions of sensors 1-5 are $(-20,25,0)$, $(-20,-25,0)$, $(20,25,0)$, $(20,-25,0)$, and $(0,0,0)$, respectively. A UAV moves through a surveillance area with the initial position of $(-10,-20,0)$, the initial velocity of $(3,5,2)^T$ and the acceleration of $u=(-0.01,-0.03,-0.04)^T$. The initial state and covariance are set as $x_0=[-10\ \ 3\ \ -20\ \ 5\ \ 0\ \ 2]^T$ and $P_0=0.01I_{6\times6}$, respectively. Set the sampling period to $T=0.1s$. The process noise covariance and the measurement noise covariance are set as $Q=0.5I_{6\times6}$ and $R=0.01I_{4\times4}$, respectively. The parameters of the relays are set to $P_s=2.3$, $P_r=3.4$, $C_s=0.35I_{4\times4}$, $C_r=0.35I_{4\times4}$, $R_s=0.08I_{4\times4}$ and $R_r=0.08I_{4\times4}$. Other parameters are taken as $\varepsilon_1=0.07$, $\varepsilon_2=0.05$, $\varepsilon_3=0.1$, $\gamma_1=\gamma_2=1$. It is worth noting that these parameters need to be set according to the actual situation in engineering applications. In addition, a trial-and-error method is adopted for selecting parameters related to these cross-terms [43].

In addition, the mean square error (MSE) is used to assess the filtering accuracy of target positioning, aiming to demonstrate the superiority of this filtering algorithm. Let $E_p=\frac{1}{N}\sum_{\lambda=1}^{N}\sum_{i=1}^{n}(x_{i,k}-\hat{x}_{i,k})^2$ represent the MSE of the target location estimation where $N=100$ denotes the number of Monte Carlo trials, $n=3$ denotes the dimensions of the coordinates, and $\hat{x}_{i,k}$ is the estimation of $x_{i,k}$.

To assess the proposed algorithm's resilience to outliers, the REKF scheme is compared with the EKF scheme in scenarios involving measurements affected by substantial measurement noises across multiple sampling periods.

Case 1: From $k=10$ to $k=30$, measurements at every ten sampling moments are contaminated by an additive noise $\varpi_k \sim N(5,2)$.

Case 2: From $k=30$ to $k=60$, measurements at every ten sampling moments are contaminated by an additive noise $\varpi_k \sim N(10,2)$.

Case 3: From $k=60$ to $k=100$, measurements at every ten sampling moments are contaminated by an additive noise $\varpi_k \sim N(15,2)$.

Fig. 2 shows the four-dimensional TDOA measurements affected by amplitude random outliers. The pronounced presence of outliers inevitably leads to substantial disruption in the innovations, adversely affecting estimation accuracy. The purpose of the designed estimator is to mitigate the impact of these "harmful" innovations by constraining them within a specified range, defined by the saturation bound.

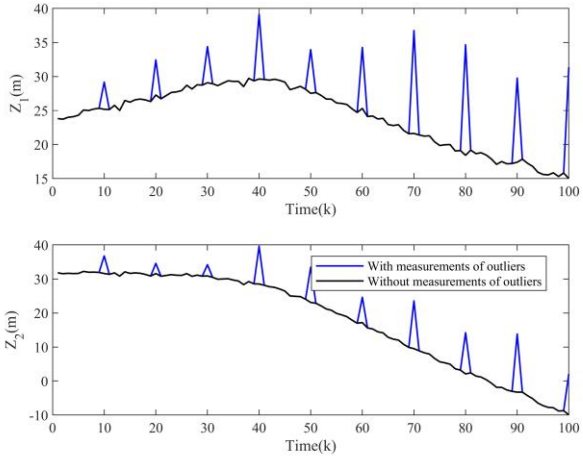

(a)

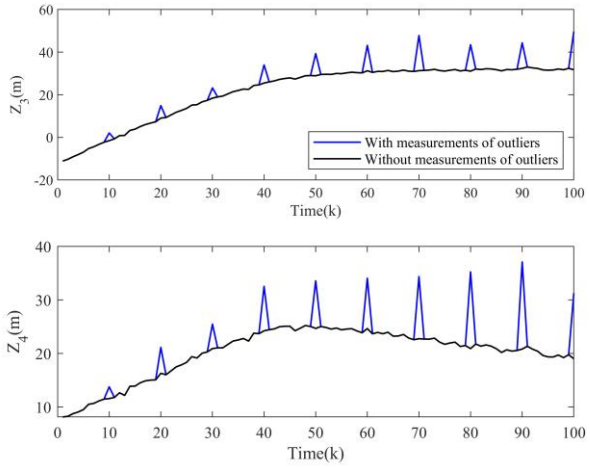

(b)

Fig. 2. Measurements under the influence of amplitude random outliers. (a) Z_1 and Z_2, (b) Z_3 and Z_4.

Fig. 3 depicts the 3D motion trajectory of the UAV and the position tracking curves of both EKF and the designed REKF in the presence of measurement outliers and the AF relaying strategy. Compared to the EKF estimator, the designed REKF exhibits higher estimation accuracy, attributed to the reduced impact of outliers on the measurements, while accounting for higher-order term error.

Fig. 4 illustrates the upper bound of the filtering error covariance and the MSE for both the EKF estimator and the designed REKF. Through a comparative analysis of the results, it is evident that the designed REKF estimator yields a lower filtering error compared to the EKF estimator. This reduction in the effect of outliers enables more accurate tracking of the UAV position.

Figs. 5-7 present the actual trajectories of the x, y, and z-axes, respectively. The figures also display the position estimates derived from both the standard filter and the designed filter, illustrating the superior estimation accuracy of the designed filter. It is noteworthy that the z-axis estimation is comparatively less accurate than the x and y-axes, attributed to a higher correlation between the estimation accuracy and the target altitude.

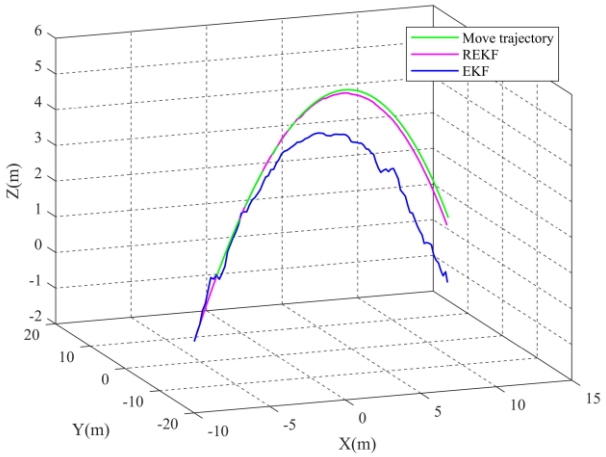

Fig. 3. UAV movement trajectory and estimated trajectory.

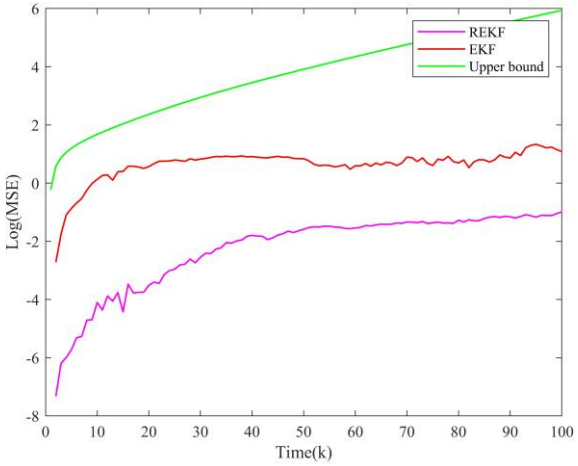

Fig. 4. MSE of different state estimators.

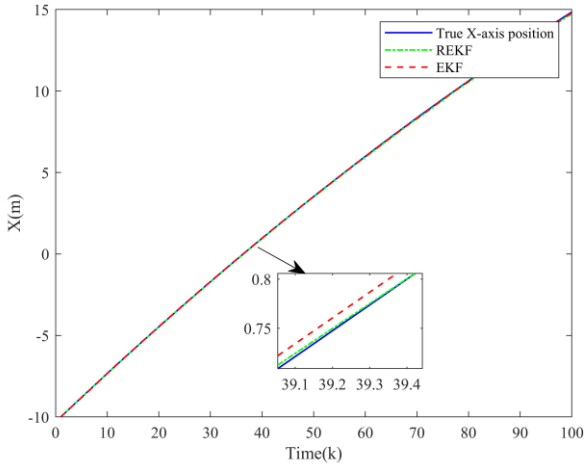

Fig. 5. UAV X-axis position and estimation.

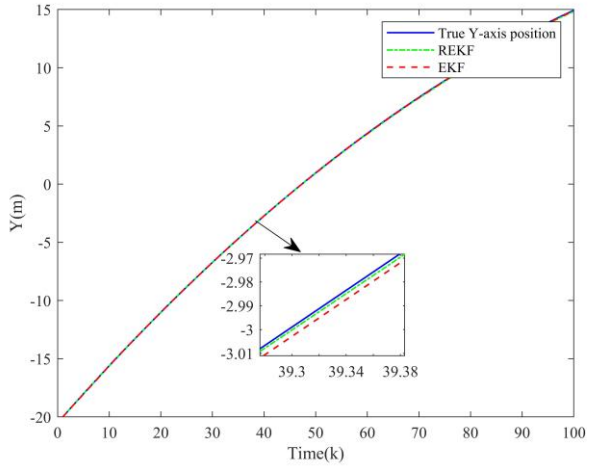

Fig. 6. UAV Y-axis position and estimation.

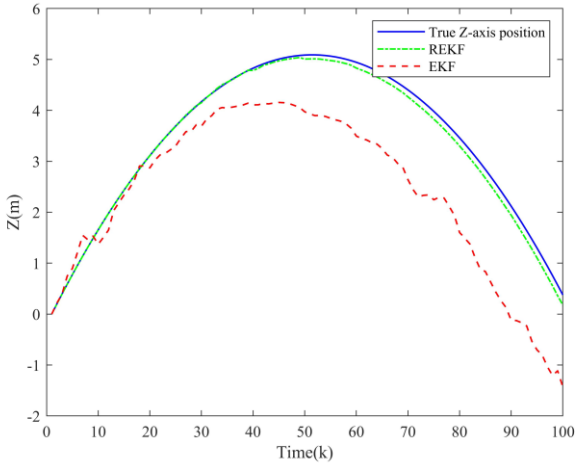

Fig. 7. UAV Z-axis position and estimation.

To address the impact of different hibernation saturation constraint bounds on tracking performance, Figs. 8-9 are presented with saturation value sets to three different levels, respectively. In Fig. 8, it is evident that lower saturation bounds impose more pronounced constraints on anomalous innovations, resulting in higher tracking accuracy. Fig. 9 shows the MSE of state estimation under varying saturation bounds. When $0 < k < 30$, all three saturation bound sets can effectively mitigate the negative impacts caused by the anomalous innovations, with minor differences attributed to the lower amplitude of wild values. However, when $k > 30$, the differences become more significant, correlating with higher amplitude outliers, and lower saturation bounds correspond to lower MSE. The presence of outliers affects estimate accuracy by influencing innovations when measurement outliers are present. The proposed saturation function mitigates the effect of outliers to some extent by operating on innovations and restricting them to the saturation value.

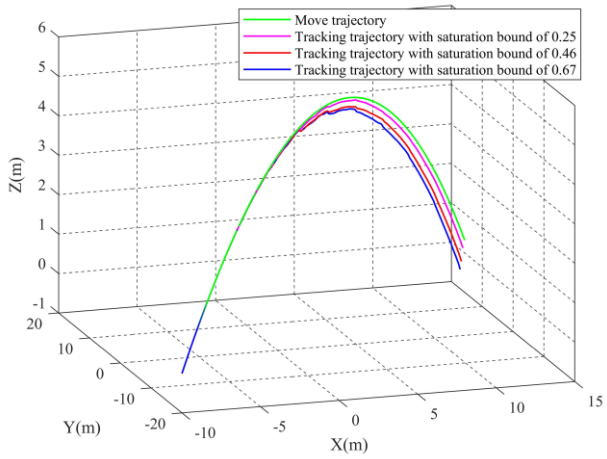

Fig. 8. UAV movement trajectory and estimated trajectory with different saturation values.

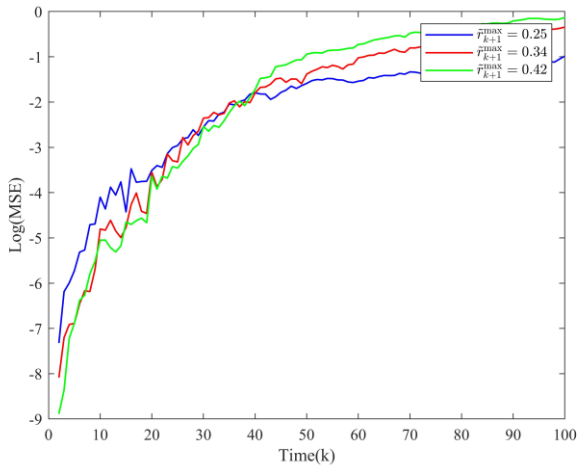

Fig. 9. MSE with different saturation values.

Through theoretical and experimental validation, the proposed method offers online application capabilities and significant potential for UAV applications in rescue search missions and environmental detection. It is important to emphasize that the implementation of the proposed positioning algorithms and the execution of UAV rescue operations depend on a myriad of practical engineering factors [44].

Remark 8: The proposed solution effectively tackles challenges related to AF relaying strategies and measurement outliers, ensuring positioning accuracy for UAVs during rescue operations. It is noted that the time complexities for solving variables $x_{k+1|k}$, $\bar{\Xi}_{k+1|k}$, K_{k+1}, $x_{k+1|k+1}$ and $\bar{\Xi}_{k+1|k+1}$ are represented as $O(n^2+nm)$, $O(n^3)$, $O(n^3+m^3)$, $O(nm)$, and $O(n^3+m^3)$, respectively. With $m<n$ in this study, the algorithm's time complexity is denoted by $O(n^3)$ [45]. In such scenarios, leveraging the advanced computing capabilities of the remote control center can mitigate excessive computational demands. Despite all this, it is essential to acknowledge certain implementation and procedural complexities: 1) Resource constraints, like energy and

communication bandwidth constraints, present inherent challenges in practical engineering [46]; 2) Diverse environmental factors, such as quantization effects, packet loss, and delays, can affect algorithm performance [47]; and 3) Ensuring security and privacy protection is critical during data transmission and processing [48]. By addressing these challenges and incorporating innovative strategies, we strive to further improve the effectiveness and reliability of our UAV positioning system for rescue missions in forthcoming studies.

V. Conclusion

In this paper, the problem of UAV target tracking has been investigated within the context of wireless positioning systems, considering the presence of AF relays and measurement outliers. The relaying strategy has been utilized to enhance the quality of transmissions for UAV measurement signals. To mitigate the impact of outliers on measurement innovations, an outlier-resistant structure has been introduced, incorporating a saturation function. Leveraging the mathematical induction method, an outlier-resistant REKF algorithm has been developed to ensure robust filtering performance. The designed filtering algorithm has been simulated in real-time UAV positioning, demonstrating its capability for accurate tracking of rescue UAVs. Future research endeavors mainly include: 1) Optimization of UAV energy management systems, exploration of sustainable and efficient energy charging solutions, and intensive research on UAV positioning challenges within energy-constrained environments; and 2) UAV-mounted intelligent reflecting surfaces for reflecting target location and orientation information to assist wireless sensor systems in target positioning [49]-[51].

References

[1] P. Paikrao, S. Routray, A. Mukherjee, A. R. Khan, and R. Vohnout, Consumer personalized gesture recognition in UAV-based industry 5.0 applications, *IEEE Transactions on Consumer Electronics*, vol. 69, no. 4, pp. 842-849, 2023.

[2] P. Du, Y. Shi, H. Cao, S. Garg, G. Kaddoum, and M. Alrashoud, 3D trajectory optimization and communication resources allocation in UAV-assisted IoT networks for sustainable industry 5.0, *IEEE Transactions on Consumer Electronics*, in press, DOI:10.1109/TCE.2023.3325131.

[3] A. Ranjha, M. A. Javed, M. J. Piran, M. Asif, M. Hussien, S. Zeadally, and J. Frnda, Towards facilitating power efficient URLLC systems in UAV networks under jittering, *IEEE Transactions on Consumer Electronics*, in press, DOI:10.1109/TCE.2023.3305550.

[4] Y. Shen, J. Huang, D. Chen, J. Wang, J. Li, and V. Ferreira, An automatic framework for pylon detection by a hierarchical coarse-to-fine segmentation of powerline corridors from UAV LiDAR point clouds, *International Journal of Applied Earth Observation and Geoinformation*, vol. 118, art.no. 103263, 2023.

[5] H. Luo, T. Chen, X. Li, S. Li, C. Zhang, G. Zhao, and X. Liu, KeepEdge: A knowledge distillation empowered edge intelligence framework for visual assisted positioning in UAV delivery, *IEEE Transactions on Mobile Computing*, vol. 22, no. 8, pp. 4729-4741, 2023.

[6] K. Liu and J. Zheng, UAV trajectory optimization for time-constrained data collection in UAV-enabled environmental monitoring systems, *IEEE Internet of Things Journal*, vol. 9, no. 23, pp. 24300-24314, 2022.

[7] C. Hu, G. Qu, H.-S. Shin, and A. Tsourdos, Distributed synchronous cooperative tracking algorithm for ground moving target in urban by UAVs, *International Journal of Systems Science*, vol. 52, no. 4, pp. 832-847, 2021.

[8] K. Messaoudi, O. S. Oubbati, A. Rachedi, A. Lakas, T. Bendouma, and N. Chaib, A survey of UAV-based data collection: Challenges, solutions and future perspectives, *Journal of Network and Computer Applications*, vol. 216, art.no. 103670, 2023.

[9] T. Bouzid, N. Chaib, M. L. Bensaad, and O. S. Oubbati, 5G network slicing with unmanned aerial vehicles: Taxonomy, survey, and future directions, *Transactions on Emerging Telecommunications Technologies*, vol. 34, no. 3, art.no. e4721, 2023.

[10] D. Perez-Saura, M. Fernandez-Cortizas, R. Perez-Segui, P. Arias-Perez, and P. Campoy, Urban firefighting drones: Precise throwing from UAV, *Journal of Intelligent and Robotic Systems*, vol. 108, art.no. 66, 2023.

[11] K. Guo, X. Li, and L. Xie, Ultra-wideband and odometry-based cooperative relative localization with application to multi-UAV formation control, *IEEE Transactions on Cybernetics*, vol. 50, no. 6, pp. 2590-2603, 2020.

[12] E. Mostafa, L. Fu, A. Ibrahim.I., and A. Usman, A solution of UAV localization problem using an interacting multiple nonlinear fuzzy adaptive H∞ models filter algorithm, *Chinese Journal of Aeronautics*, vol. 32, no. 4, pp. 978-990, 2019.

[13] A. Beishenalieva and S.-J. Yoo, Multiobjective 3-D UAV movement planning in wireless sensor networks using bioinspired, *IEEE Internet of Things Journal*, vol. 10, no. 9, pp. 8096-8110, 2023.

[14] J. Y. Lee, A. Y. Chung, H. Shim, C. Joe, S. Park, and H. Kim, UAV flight and landing guidance system for emergency situations, *Sensors*, vol. 19, art.no. 4468, 2019.

[15] S. Chen, F. Hu, Z. Chen, and H. Wu, Correction method for UAV pose estimation with dynamic compensation and noise reduction using multi-sensor fusion, *IEEE Transactions on Consumer Electronics*, in press, DOI:10.1109/TCE.2023.3339729.

[16] P. Chanak and I. Banerjee, Congestion free routing mechanism for IoT-enabled wireless sensor networks for smart healthcare applications, *IEEE Transactions on Consumer Electronics*, vol. 66, no. 3, pp. 223-232, 2020.

[17] B. Qu, Z. Wang, B. Shen, and H. Dong, Distributed state estimation for renewable energy microgrids with sensor saturations, *Automatica*, vol. 131, art.no. 109730, 2021.

[18] S. Li, C. Gao, M. Wei, J. Zhao, P. Shao, and J. Xu, CSI-impaired secure resource allocation for SWIPT-enabled full-duplex consumer internet of things networks in smart healthcare, *IEEE Transactions on Consumer Electronics*, vol. 69, no. 4, pp. 685-696, 2023.

[19] H. Li and A. V. Savkin, Wireless sensor network based navigation of micro flying robots in the industrial internet of things, *IEEE Transactions on Industrial Informatics*, vol. 14, no. 8, pp. 3524-3533, 2018.

[20] P. Sinha and I. Guvenc, Impact of antenna pattern on TOA based 3D UAV localization using a terrestrial sensor network, *IEEE Transactions on Vehicular Technology*, vol. 71, no. 7, pp. 7703-7718, 2022.

[21] X. Bai, Z. Wang, L. Zou, and Z. Zhang, Target tracking for wireless localization systems using set-membership filtering: A component-based event-triggered mechanism, *Automatica*, vol. 132, art.no. 109795, 2021.

[22] A. Rajagopal and S. Chitraganti, State estimation and control for networked control systems in the presence of correlated packet drops, *International Journal of Systems Science*, vol. 54, no. 11, pp. 2352-2365, 2023.

[23] W. Qian, W. Xing, and S. Fei, H∞ state estimation for neural networks with general activation function and mixed time-varying delays, *IEEE Transactions on Neural Networks and Learning Systems*, vol. 32, no. 9, pp. 3909-3918, 2021.

[24] K. J. Uribe-Murcia and Y. S. Shmaliy, Robust UFIR observer for WSNs with multistep random delays and multiple packet dropouts, *IEEE Transactions on Automatic Control*, vol. 68, no. 10, pp. 6338-6344, 2023.

[25] J. Khalife and Z. M. Kassas, Opportunistic UAV navigation with carrier phase measurements from asynchronous cellular signals, *IEEE Transactions on Aerospace and Electronic Systems*, vol. 56, no. 4, pp. 3285-3301, 2020.

[26] Z. Qiu, S. Wang, P. Hu, and L. Guo, Outlier-robust extended Kalman filtering for bioinspired integrated navigation system, *IEEE Transactions on Automation Science and Engineering*, in press, DOI:10.1109/TASE.2023.3319508.

[27] X. Bai, Z. Wang, L. Zou, and C. Cheng, Target tracking for wireless localization systems with degraded measurements and quantization effects, *IEEE Transactions on Industrial Electronics*, vol. 65, no. 12, pp. 9687-9697, 2018.

[28] W. Qian, D. Lu, S. Guo, and Y. Zhao, Distributed state estimation for mixed delays system over sensor networks with multichannel random attacks and Markov switching topology, *IEEE Transactions on Neural Networks and Learning Systems*, in press, DOI:10.1109/TNNLS.2022.3230978.
[29] L. Ma, Z. Wang, J. Hu, and Q.-L. Han, Probability-guaranteed envelope-constrained filtering for nonlinear systems subject to measurement outliers, *IEEE Transactions on Automatic Control*, vol. 66, no. 7, pp. 3274-3281, 2021.
[30] B. Qu, Z. Wang, B. Shen, and H. Dong, Decentralized dynamic state estimation for multi-machine power systems with non-Gaussian noises: Outlier detection and localization, *Automatica*, vol. 153, art.no. 111010, 2023.
[31] H. Fang, M. A. Haile, and Y. Wang, Robust extended Kalman filtering for systems with measurement outliers, *IEEE Transactions on Control Systems Technology*, vol. 30, no. 2, pp. 795-802, 2022.
[32] L. Zou, Z. Wang, J. Hu, and H. Dong, Partial-node-based state estimation for delayed complex networks under intermittent measurement outliers: A multiple-order-holder approach, *IEEE Transactions on Neural Networks and Learning Systems*, vol. 34, no. 10, pp. 7181-7195, 2023.
[33] W. Qian, Y. Li, Y. Chen, and W. Liu, L2-L∞ infinity filtering for stochastic delayed systems with randomly occurring nonlinearities and sensor saturation. *International Journal of Systems Science*, vol. 51, no. 13, pp. 2360–2377, 2020.
[34] L. Zou, Z. Wang, B. Shen, and H. Dong, Moving horizon estimation over relay channels: Dealing with packet losses, *Automatica*, vol. 155, art.no. 111079, 2023.
[35] Y. Liu, Z. Wang, H. Lin, L. Ma, and G. Lu, Encoding–decoding-based fusion estimation with filter-and-forward relays and stochastic measurement delays, *Information Fusion*, vol. 100, art.no. 101963, 2023.
[36] T. M. Hoang, L. T. Dung, B. C. Nguyen, X. N. Tran, and T. Kim, Secrecy performance analysis for MIMO-DF relay systems with MRT/MRC and TZF/MRC schemes, *IEEE Transactions on Vehicular Technology*, vol. 72, no. 8, pp. 10173-10186, 2023.
[37] M. A. Hasabelnaby and A. Chaaban, Multi-pair computation for two-way intra cloud radio-access network communications, *IEEE Transactions on Wireless Communications*, vol. 21, no. 7, pp. 5586-5599, 2022.
[38] V. Navratil, J. Krska, and F. Vejrazka, Concurrent bidirectional TDOA positioning in UWB network with free-running clocks, *IEEE Transactions on Aerospace and Electronic Systems*, vol. 58, no. 5, pp. 4434-4450, 2022.
[39] H. Tan, B. Shen, K. Peng, and H. Liu, Robust recursive filtering for uncertain stochastic systems with amplify-and-forward relays, *International Journal of Systems Science*, vol. 51, no. 7, pp. 1188-1199, 2020.
[40] W. Song, J. Wang, S. Zhao, and J. Shan, Event-triggered cooperative unscented Kalman filtering and its application in multi-UAV systems, *Automatica*, vol. 105, pp. 264-273, 2019.
[41] L. Xie, Y. C. Soh, and C. E. de Souza, Robust Kalman filtering for uncertain discrete-time systems, *IEEE Transactions on Automatic Control*, vol. 39, no. 6, pp. 1310-1314, 1994.
[42] Y. Liu, Z. Wang, C. Liu, M. Coombes, and W.-H. Chen, Auxiliary particle filtering over sensor networks under protocols of amplify-and-forward and decode-and-forward relays, *IEEE Transactions on Signal and Information Processing over Networks*, vol. 8, pp. 883-893, 2022.
[43] B. Qu, Z. Wang, B. Shen, and H. Dong, Outlier-resistant recursive state estimation for renewable-electricity-generation-based micro-grids, *IEEE Transactions on Industrial Informatics*, vol. 19, no. 5, pp. 7133-7144, 2023.
[44] R. A. Qamar, M. Sarfraz, A. Rahman, and S. A. Ghauri, Multi-criterion multi-UAV task allocation under dynamic conditions, *Journal of King Saud University - Computer and Information Sciences*, vol. 35, art.no. 101734, 2023.
[45] C. Lu, S. Wu, C. Jiang, and J. Hu, Weak harmonic signal detection method in chaotic interference based on extended Kalman filter, *Digital Communications and Networks*, vol. 5, no. 1, pp. 51-55, 2019.
[46] J.-Y. Li, Z. Wang, R. Lu, and Y. Xu, Distributed filtering under constrained bit rate over wireless sensor networks: Dealing with bit rate allocation protocol, *IEEE Transactions on Automatic Control*, vol. 68, no. 3, pp. 1642-1654, 2023.
[47] R. Kumada and K. Adachi, Interference cancelation for coexistence of LoRaWAN with wireless power transfer, *IEEE Internet of Things Journal*, vol. 10, no. 15, pp. 13109-13122, 2023.
[48] C. Gao, Z. Wang, X. He, and H. Dong, Fault-tolerant consensus control for multiagent systems: An encryption-decryption scheme, *IEEE Transactions on Automatic Control*, vol. 67, no. 5, pp. 2560-2567, 2022.
[49] P. Wang, W. Mei, J. Fang, and R. Zhang, Target-mounted intelligent reflecting surface for joint location and orientation estimation, *IEEE Journal on Selected Areas in Communications*, vol. 41, no. 12, pp. 3768-3782, 2023.
[50] X. Pang, W. Mei, N. Zhao, and R. Zhang, Cellular sensing via cooperative intelligent reflecting surfaces, *IEEE Transactions on Vehicular Technology*, vol. 72, no. 11, pp. 15086-15091, 2023.
[51] W. Nie, Z.-C. Han, Y. Li, W. He, L.-B. Xie, X.-L. Yang, and M. Zhou, UAV detection and localization based on multi-dimensional signal features, *IEEE Sensors Journal*, vol. 22, no. 6, pp. 5150-5162, 2022.

Xingzhen Bai received the B.Sc. degree in electrical technology and the M.Sc. degree in power electronics and power drives from the Shandong University of Science and Technology, Qingdao, China, in 2000 and 2006, respectively, and the Ph.D. degree in computer software and theory from Tongji University, Shanghai, China, in 2010. He is currently a Professor with the College of Electrical Engineering and Automation, Shandong University of Science and Technology. His current research interests include distributed estimation and control, wireless sensor network, and smart grid.

Liqun Yu received the B.Sc. degree in automation from the College of Electrical Engineering and Automation, Shandong University of Science and Technology, Qingdao, China, in 2022. She is currently pursuing the M.Sc. degree in electrical engineering from the Shandong University of Science and Technology, Qingdao, China.

Guhui Li received the B.Sc. degree in electrical engineering and automation from the College of Electrical Engineering and Automation, Qilu University of Technology, Jinan, China, in 2020, and the M.Sc. degree in electrical engineering from the Shandong University of Science and Technology, Qingdao, China, in 2023, where he is currently pursuing the Ph.D. degree in control science and engineering. His current research interests include distributed estimation and control and its application in power distribution networks.

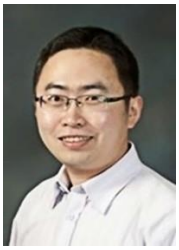

Lu Liu received his MSc degree in data communication systems from Brunel University (UK) in 2003 and his PhD degree from the University of Surrey (UK) in 2008. He is a Professor of Artificial Intelligence at the University of Exeter (UK). His research interests are in the areas of Artificial Intelligence, Data Science, Sustainable Systems and the Internet of Things. He is a Fellow of British Computer Society (BCS).

Xiao Chen holds MSc and PhD degrees in computing science from Newcastle University (UK) and currently serves as a lecturer in the School of Computing and Mathematical Sciences at the University of Leicester. Previously, he was a Marie Skłodowska-Curie fellow at the School of Informatics at the University of Edinburgh (UK). His research interests revolve around the theory of distributed systems, blockchains, and consensus protocols, with a focus on blockchain-supported distributed AI systems. Additionally, he specialises in stochastic and formal modelling, as well as AI-driven optimisation for large-scale systems.